Biosensors

DOI: 10.1002/ange.201006469

Single-Molecule Detection of Proteins Using Aptamer-Functionalized Molecular Electronic Devices**

Song Liu, Xinyue Zhang, Wangxi Luo, Zhenxing Wang, Xuefeng Guo, Michael L. Steigerwald, and Xiaohong Fang**

Dedicated to Professor Daoben Zhu on the occasion of his 70th birthday

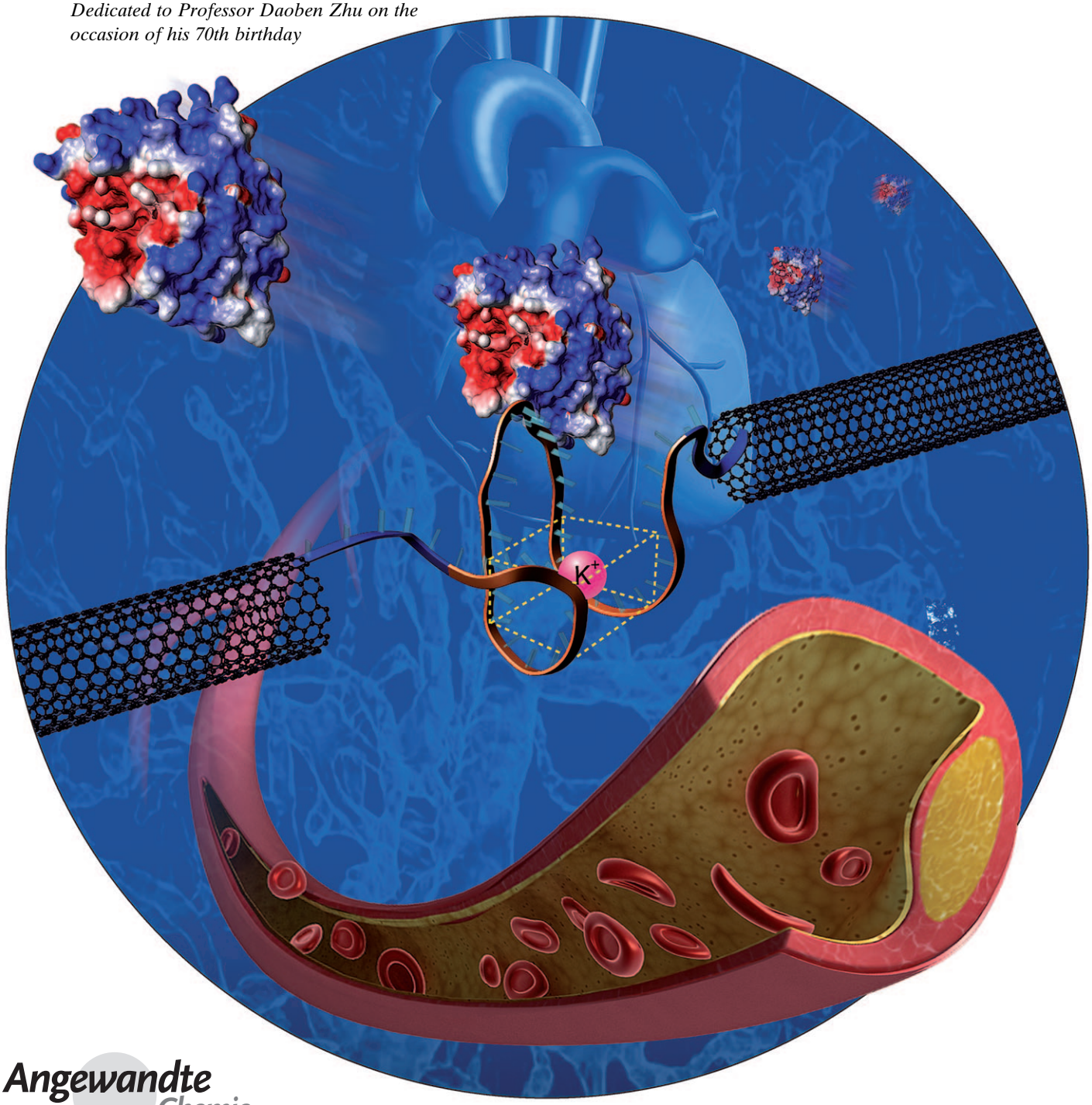

Establishing a practical platform for directly detecting the activities of biological and chemical species at the single-molecule level is one of the ultimate goals in both the scientific and industrial communities for a wide variety of applications, including environmental monitoring, industrial quality control, and clinical diagnostics.[1] Several label-based or label-free techniques have been demonstrated to achieve the reliable detection of proteins, including the enzyme-linked immunosorbent assay (ELISA),[2a] surface plasmon resonance (SPR),[2b] electrochemistry,[2c,d] scanning probe microscopy (SPM),[2e] impedance spectroscopy[2f] and assays with enhanced sensitivity employing nanoparticles,[2g] microcantilevers,[2h] carbon nanotubes,[2i] and nanowires.[2j] However, some of the detection approaches developed so far are not suitable for real-time detection and/or kinetic analysis; some suffer from overly sophisticated technical requirements; and others lack high sensitivity and selectivity. An optimized strategy would create an integrated system that can combine rapid real-time measurements with sensitivity, selectivity, and reversibility, and would be able to monitor individual binding events.[3]

Previously, we developed a lithographic method to covalently wire one or a few molecules onto both facing ends of nanogaps in carbon nanotubes by means of amide linkages for building functional single-molecule devices.[4] This approach avoids the problems commonly associated with suspending DNAs between electrodes which yields a broad spectrum of DNA conductance behaviors from insulating to superconductive (see Ref. [5] and references therein). Furthermore, in this system, the devices were sufficiently robust that a wide range of chemistries and conditions could be applied. By using this method we have made molecular devices that function as scaffolding for the assembly of multicomponent nanostructures,[6a] and that probe the charge-transport dependence of a single intact DNA duplex on π-stacking integrity.[6b,7] Herein, we report a reliable system, a crucial test for practical applications, in which individual DNA aptamers were coupled with single-walled carbon nanotubes (SWNTs) at point contacts to form single-molecule devices, which allow us to selectively and reversibly detect a single specific analyte, thrombin, in real time (Figure 1 a,b). We used aptamers because they are single-stranded nucleic acid ligands that have been engineered through repeated rounds of in vitro selection to strongly and selectively bind to various molecular targets from small molecules to proteins, even to whole cells. Aptamers are antibody-like molecules in that they function primarily in molecular recognition. In contrast to antibodies for the detection of target proteins, aptamers are advantageous in their quick and reproducible synthesis, easy and controllable chemical modification, long-term stability, and ability to sustain reversible denaturation. They are emerging as ideal recognition elements in a number of biosensing platforms, especially in protein detection.[1b,d,5,8]

The "nanogapped" SWNTs are fabricated by a method described in detail elsewhere.[4,6] Figure 1 c shows the scanning electron microscopy (SEM) and tapping-mode atomic force microscopy (AFM) images of the devices used. This gap is too small to be seen by SEM (Figure 1 c), but it can be located and directly imaged with AFM. For the high-resolution AFM micrograph in Figure 1 c, we take the imaging convolution of the AFM tip size into account and set an upper bound on the size of a typical gap opened in the SWNTs of roughly 10 nm (the diameter of the tube is approximately 1.2 nm). It is in this gap that we have made a number of different molecular electronic devices. We reconnected the carbon nanotube ends with single aptamer molecules terminated with amine groups using a two-step strategy.[6b] The 15-mer thrombin aptamer with thymine 7 (T7) linkers on both the 3′ and 5′ termini (Apt-A) was used to construct the protein-detection device. This aptamer assumes a G4 conformation when it binds with the target human α-thrombin, and the binding affinity is high ($K_d \approx 2.8$ nM). Another 15-mer random oligonucleotide sequence with T7 linkers on both sides, which could not bind human α-thrombin, was used as a control (Con-A). Experimental details on device fabrication, device reconnection, and thrombin treatment can be found in the Supporting Information.

Figure 1 d shows the comparison of current–voltage (I–V) curves for a representative device rejoined by Apt-A. The black curve shows the source-drain current (I_D) as a function of the gate voltage (V_G) at a constant source-drain bias (V_D) of −50 mV for the pristine nanotube. Before cutting, this SWNT without the gap is a *p*-type semiconducting device. After cutting and initial treatment of the gap with coupling agents, the device shows no measurable current at the noise level of the measurement (< 50 fA, red curve). The green curve in Figure 1 d illustrates the conductance of the same device after reconnection with amine-modified Apt-A. We found that all the reconnected carbon nanotube devices, including the device shown in Figure 1 d, recover their original (either *p*-type semiconducting or metallic) properties. We note that the gate voltage that can be applied to the reconnected devices is limited. At higher gate biases (> 6 V),

[*] S. Liu,[+] Z. Wang, Prof. X. Guo
Beijing National Laboratory for Molecular Sciences
State Key Laboratory for Structural Chemistry of Unstable and Stable Species, College of Chemistry and Molecular Engineering
Peking University, Beijing 100871 (P. R. China)
Fax: (+86) 10-6275-7789
E-mail: guoxf@pku.edu.cn
X. Zhang,[+] W. Luo, Prof. X. Fang
Beijing National Laboratory for Molecular Sciences
Institute of Chemistry, Chinese Academy of Sciences
Beijing 100190 (P. R. China)
E-mail: xfang@iccas.ac.cn
Dr. M. L. Steigerwald
Department of Chemistry and the Columbia University Center for Electronics of Molecular Nanostructures, New York (USA)
[+] These authors contributed equally to the work.

[**] We thank Colin Nuckolls (Columbia University) and Zhongfan Liu (Peking University) for enlightening discussions. We acknowledge primary financial support from MOST (2009CB623703, 2007CB935601, 2011CB911001, and 2008AA062503), NSFC (50873004, 50821061, 20821003, and 20833001), FANEDD (2007B21), 111 Project (B08001), and BSTSP (2009A01)
Supporting information for this article is available on the WWW under http://dx.doi.org/10.1002/anie.201006469.

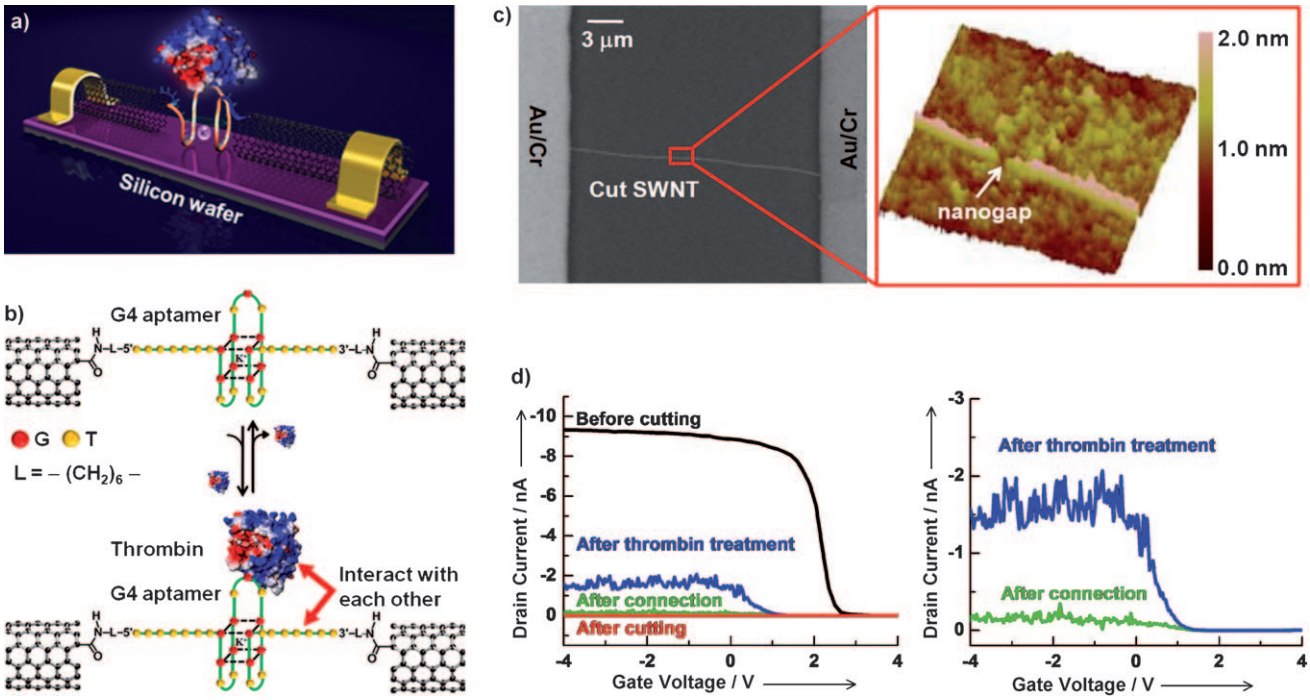

Figure 1. a) Representation of the device structure. b) Schematic representation of the sensing mechanism showing how single-molecule devices can detect proteins at the single-molecule level. c) SEM and tapping-mode AFM images of an individual SWNT after oxidative cutting. The size of the gap opened in the SWNT is typically <10 nm. The diameter of the SWNT is roughly 1.2 nm, as estimated from the height profile. The AFM image is 500 nm × 500 nm in size. d) Device characteristics of a representative device rejoined by Apt-A before cutting (black), after cutting (red), after DNA connection (green), and after treatment with 260 nM thrombin (blue). $V_D = -50$ mV. The plot on the right shows *I*–*V* curves after DNA connection and thrombin treatment with an expanded *y* scale.

the DNA bridges became less and less conductive over time until, ultimately, device breakdown was observed with the current level down to the noise level of the measurement (see Figure S1 in the Supporting Information). This is consistent with previous observations[6b] and probably arises from a hydration layer of water around the devices. To rule out the possibility of ionic conduction in devices, we treated a working device rejoined by Apt-A with different buffer solutions (PBS buffer solution, pH 7.2; Tris-HCl solution, pH 8.3) and tested the electrical properties. In both cases there was no obvious change in conductivity of the device after treatment (see Figure S2 in the Supporting Information). Table S1 summarizes the device characteristics measured in the course of this study for the devices at each step of the procedure. Using this method we obtained 14 reconnected devices out of the roughly 500 that were tested.

One important feature of Apt-A is the formation of G4 conformation itself, which can be significantly stabilized by metal ions, such as K^+ or Mg^{2+}, at room temperature.[9a] We postulate that the native G4 conformation is formed after reconnection because the PBS buffer solution used for connection reaction contains 12 mM of K^+ ions. This was further supported by control experiments, in which we treated the rejoined device by Apt-A with solutions containing 20 mM of either K^+ or Mg^{2+} ions. No obvious changes in conductivity of the device were observed for either treatment (see Figure S3 in the Supporting Information). Given that the diameter of Apt-A with the G4 conformation (≈ 2.8 nm) is comparable to that of the SWNTs grown here (<3 nm), it is unlikely that more than one DNA aptamer can fit lengthwise within the gap.

We next tested the ability of the Apt-A bridges within the gaps to recognize and bind proteins. The newly rejoined devices were immersed in 10 μL of a Tris-HCl buffer solution containing 260 nM human α-thrombin (see the Supporting Information for more details). To maximize the sensing ability, we always chose the buffer solution at pH 8.3, in which the commercially available human α-thrombin has the strongest affinity with Apt-A.[9] Remarkably, the ON-state resistance of the device shown in Figure 1 d displayed a drastic reduction by one order of magnitude, from ≈ 300 MΩ to ≈ 30 MΩ, upon association with thrombin. This result is consistent with previous reports on nanogapped metal electrodes.[2f,10] To prove the devices' reproducibility, we measured the 14 devices listed in Table S1. Although there are variations in the conductance of the devices, the behavior of each device is essentially the same. These results show that reproducible device-to-device sensing ability was achieved. To further reduce the conductance variation of the device, atomic-level precision must be realized in the cutting procedure and variations in the DNA conformation and the contact configuration must be reduced; these are the challenges for future studies.[6b,11]

We emphasize that the drastic changes in resistance observed in the present case result from a localized, individual DNA probe that is covalently bridged into the circuit, rather than Schottky barrier modification and/or nonspecific surface adsorption.[2i,12] To rule out these potential artifacts, we

performed two sets of control experiments under the same treatment conditions as those described above. In one set of control experiments, we tested the electrical properties of pristine SWNT devices upon the sequential treatments. All the SWNT devices showed a slight increase in resistance after further thrombin treatment following the reconnection step (Figure S4 in the Supporting Information), which is consistent with previous reports where surface attachment of proteins on aptamer-functionalized uncut SWNT devices led to a current drop in the devices.[12] This phenomenon is opposite to that observed in the functionalized devices discussed above. In another set of control experiments, we performed the same operations on partially cut SWNT devices (see Figure S5 in the Supporting Information). These are devices in which SWNTs were not fully cut during the oxygen-plasma treatment. We also observed changes in the ON-state resistance in the opposite direction, as described in the above control experiments.

To investigate the selectivity of the devices, we designed two additional sets of important competitive binding experiments. In the first, we performed the same set of operations using the Apt-A-functionalized devices but substituted a different protein, elastase, for thrombin. Elastase is also a serine protease and its isoelectric point and molecular weight are similar to that of thrombin. The treatment with elastase led to an increase in resistance of the devices, most likely resulting from the nonspecific adsorption of elastase as discussed above (Figure 2a). Interestingly, after elastase had been removed with clean buffer solution, further treatment of the Apt-A-functionalized devices with thrombin caused a sharp decrease in resistance, thus demonstrating the excellent selectivity of these devices. In the second experiment, we used Con-A to form the rejoined device for thrombin detection. Con-A has no affinity with thrombin and should produce no measurable changes in the ON-state resistance. There was a small resistance increase, probably arising from the nonspecific adsorption of thrombin on the surface of SWNTs as discussed above (see Figure S6 in the Supporting Information).

What is the origin of the changes in the ON-state resistance of these reconnected devices upon treatment with thrombin? The efficiency of charge transport (CT) in DNA is intimately related to the structure of the pathways that mediate CT through π-stacking base pairs. Therefore, DNA CT is sensitive to even more subtle deviations in stacking integrity. Interactions with proteins that disturb DNA π stacks inhibit DNA CT.[5] However, in our case, the three-dimensional G4 structure of Apt-A exhibits substantial conformational flexibility. We hypothesize that DNA–thrombin interactions do not distort the G4 conformation, but instead rigidify the G4 conformation and promote tight π packing, thus enhancing DNA CT[5] (Figure 2b, Route 1).

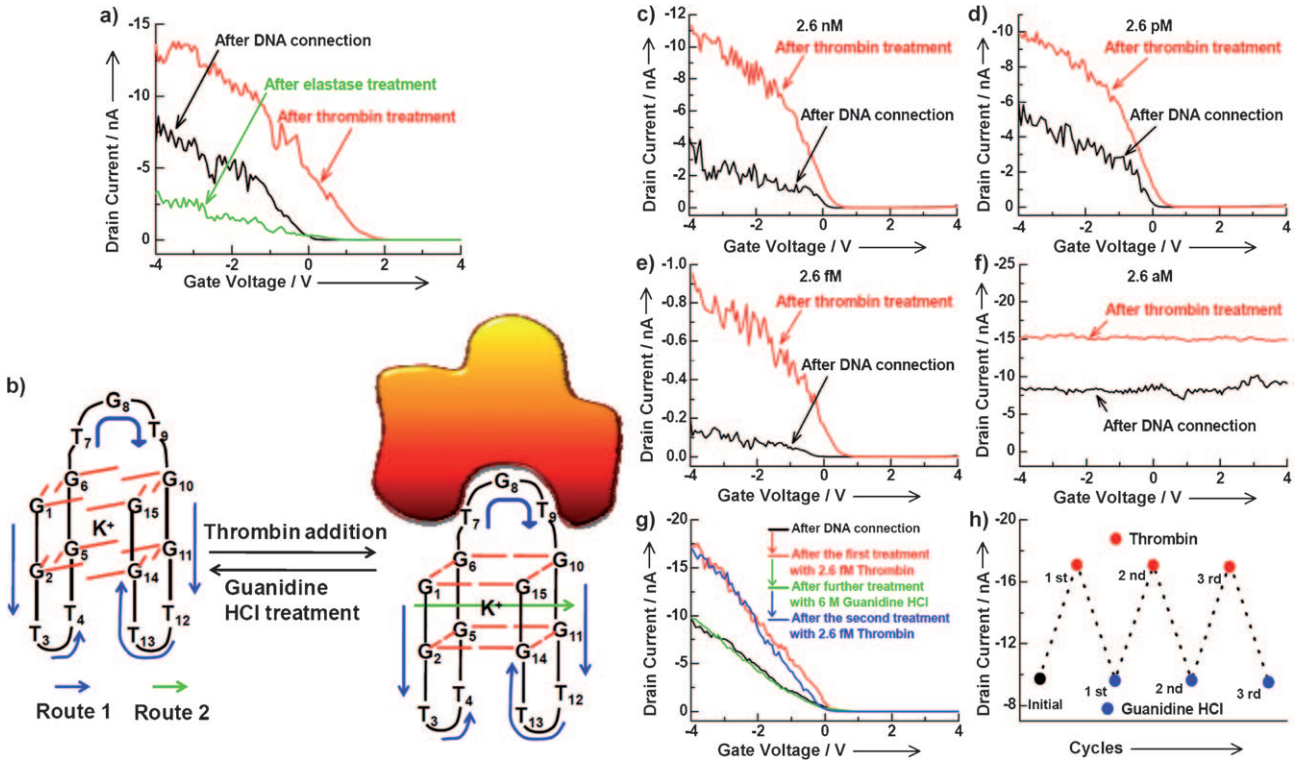

Figure 2. a) Device characteristics of a control device rejoined by Apt-A after connection (black), after elastase treatment (340 nM, green), and after thrombin treatment (260 nM, red). b) Schematic representation of sensing mechanisms showing that protein binding rigidifies the π stacking in the G4 conformation, facilitating DNA CT through Route 1 and/or Route 2. c–f) Sensitivities of different rejoined devices after DNA connection (black) and after thrombin treatment (red) at different concentrations (c: 2.6 nM, d: 2.6 pM, e: 2.6 fM, f: 2.6 aM). g) *I*–*V* curves of a reconnected device upon sequentially alternating treatment with thrombin (2.6 fM) and guanidine HCl (6 M), showing the sensing reversibility. h) Representative three switching cycles of the same device. All the measurements were performed at $V_D = -50$ mV. More details of all the devices used here can be found in Figure S7 in the Supporting Information.

This explanation is consistent with previous reports. For example, functionalization of the side chains of certain oligo(phenylene–ethynylene)s with bulky substituents can limit the conjugation-breaking torsion and thus significantly improve their conduction.[13] Another possibility is that the rigidified central guanines in the G4 conformation may provide an additional pathway for charge transport in the circuit and facilitate more efficient DNA CT (Figure 2b, Route 2). However, the experiments detailed here do not allow us to distinguish between the two mechanisms since the device might function through a combination of the two.

We next investigated the sensitivity of these reconnected devices by varying the protein concentrations. Different Apt-A-rejoined devices were used for each thrombin concentration (2.6 nM, 2.6 pM, 2.6 fM, and 2.6 aM in Tris-HCl buffer at pH 8.3). In Figure 2c–f representative *I–V* curves are shown for each case before and after thrombin treatment. Consistently, all of the working devices displayed sharp decreases in ON-state resistance to different extents, thus again demonstrating very good device-to-device absolute detection reliability and reproducibility (Table S1). We notice that the device in Figure 2 f does not show any gate dependence. This is because of the metallic property of the SWNT, indicating that the gate modulates the conductance of the nanotube more strongly than that of DNA molecules. The highest sensitivity we have tested is at least as low as 2.6 aM, approximately 88 attograms per milliliter. These results exceed those of previous protein-detection studies, in which sensitivity was much lower, for example, ELISA sandwich assays ($\approx 3\ pg\,mL^{-1}$),[2a] SPR (≈ 10–$100\ pg\,mL^{-1}$),[2b] nanowire arrays ($\approx 0.9\ pg\,mL^{-1}$),[2j] carbon nanotubes (≈ 1 pM),[2i] and microcantilevers ($\approx 0.2\ ng\,mL^{-1}$).[2h] In recent work using magnetic and gold nanoparticles[2g] sensitivity (30 aM) close to ours has been reported; however, this method requires labeling and multiple chemical and biological treatments. In principle, our devices can be employed to monitor DNA–protein interactions with single-molecule sensitivity since they have only one or at most two available binding sites for proteins.

After having established the detection selectivity and sensitivity, we turned our attention to the sensing reversibility of the devices. After immersion of a thrombin-treated device into a 6 M guanidine·HCl solution for half an hour, the conduction of the devices decreased to the initial value after DNA connection. We were fortunate to not only maintain the sensing properties of the functioning devices but also achieve good reversibility (Figure 2g). Control experiments using pristine and partially cut SWNT devices did show negligible changes in conductance under the same conditions (see Figures S4 and S5 in the Supporting Information). Importantly, the sensing process is reversible. After further thrombin treatment, the device recovered its high conductive state. Figure 2h demonstrates three representative sensing cycles of the same device shown in Figure 2g, thereby setting the foundation for cyclable real-time biodetection.

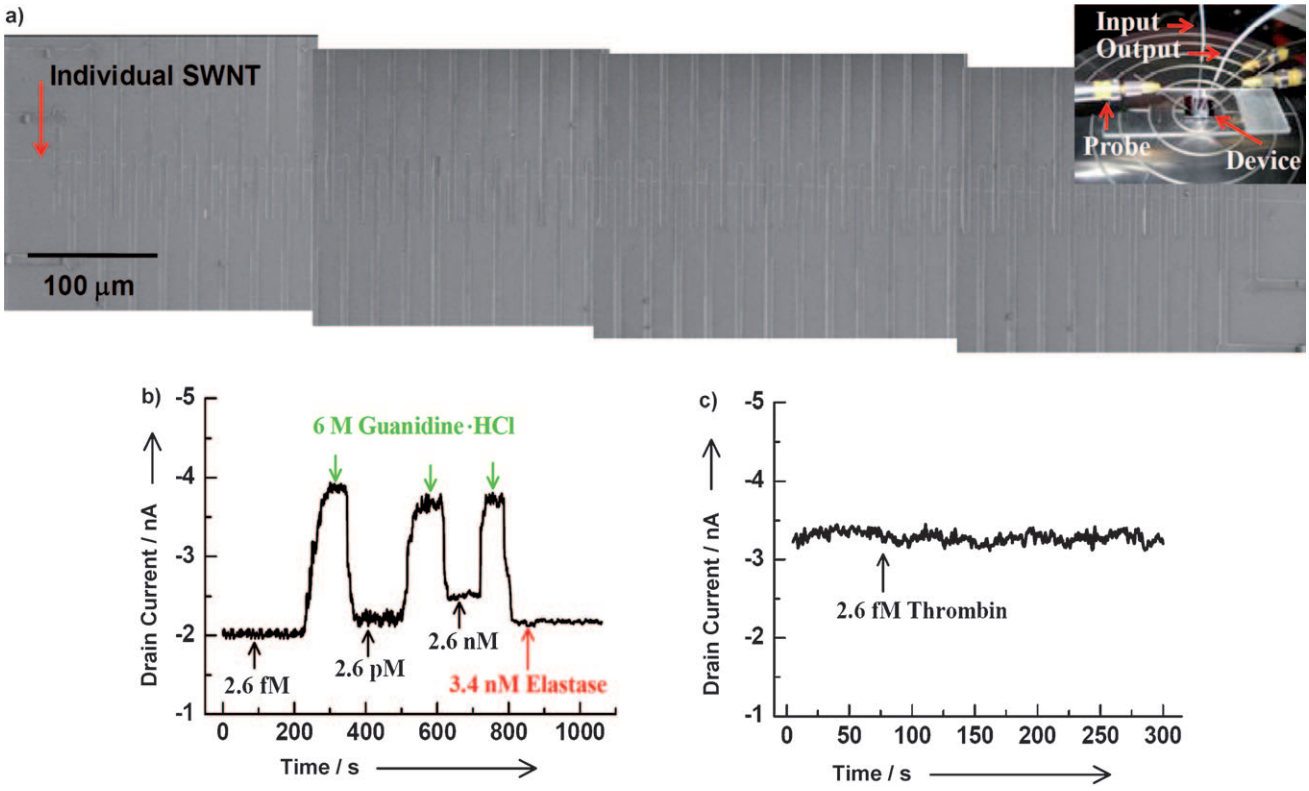

Figure 3. a) SEM images showing highly integrated identical SWNT devices. Inset shows an optical image of a single-molecule device during real-time measurements. b) Current-versus-time data recorded for an Apt-A-rejoined device upon alternate additions of the thrombin Tris-HCl buffer solution at different concentrations (from 2.6 fM to 2.6 pM and 2.6 nM), the 6 M guanidine HCl solution, and finally the elastase (3.4 nM) Tris-HCl buffer solution. c) *I–V* plot recorded for a Con-A-rejoined device upon injection of 2.6 fM thrombin in Tris-HCl buffer solution. All the measurements were performed at $V_D = -50$ mV and $V_G = 0$ V.

Finally, we developed a practical method for mass-producing high-density SWNT transistor arrays, a method that is suitable for the fabrication of single-molecule devices and real-time detection. We designed and fabricated a repeating pattern that consists of 79 identical SWNT transistors, whose metal electrodes have been passivated by 50 nm thick layer of silicon oxide, by a double photolithographic process (see the Supporting Information for more details). The series of SEM images in Figure 3a show that an individual SWNT nicely spans all 80 metal electrodes. By employing the improved methods for the fabrication of single-molecule devices described previously,[4,6] we can get, on average, two working devices out of the 79 original SWNT transistors on each chip. In combination with microfluidics (Figure 3a, inset), we are able to detect protein and monitor stochastic DNA–protein interactions in real time (Figure 3b,c). The device was stabilized by first flowing pure Tris-HCl buffer solution at a flow rate of 20 $\mu L\,min^{-1}$ for roughly 75 seconds; subsequent thrombin injection resulted in a sharp increase in conductance (Figure 3b), consistent with the results described above. Importantly, we observed very good reversible conductance changes at different thrombin concentrations (from 2.6 fM to 2.6 pM and 2.6 nM; Figure 3b). Further delivery of elastase (3.4 nM) did not lead to any detectable conductance change in the same device. Control experiments using the device reconnected with Con-A showed negligible conductance change upon thrombin injection (2.6 fM; Figure 3c). The most important thing we should emphasize is that reversible electrical measurements on the same device at different thrombin concentrations indeed showed essentially equivalent conductance changes, which distinguishes our method as a unique platform from previous reports where nanotubes and nanowires were used to detect bulky proteins with concentration dependence.[2i,j,12] The small decrease in conductance change most likely results from nonspecific surface adsorption with the increase of thrombin concentrations and/or the slight device degradation during real-time measurements. The fact that real-time detection events showed no concentration dependence proves that these devices are monitoring DNA–protein interactions at the single-event level.[14] Therefore, these results demonstrate real-time, label-free, reversible detection of DNA–protein interactions with essentially complete selectivity and real single-molecule sensitivity. The typical response time is short, within a minute, which is likely related to the convolution of the conformation dynamics during and after stochastic protein binding.

Collectively, we detail here a practical yet reliable approach in which molecular electronics are interfaced with biological systems to realize the label-free, real-time, reversible electrical detection of DNA and/or protein activities. This method uses functional single-molecule devices to achieve ultrahigh selectivity and sensitivity. We believe that this methodology can move beyond current technologies and has a wide variety of applications. These single-molecule junctions allow controllable and diverse functionalizations with specific, directed capabilities, and they detect specific activities at the single-molecule level. These capabilities may be used to address critical biological problems in living tissue and to detect traces of chemical and biological species that are detrimental to the environment. Second, the proven reliability and reproducibility of single-molecule devices and ability to integrate these hybrid devices on silicon chips, which is compatible to current complementary metal oxide semiconductor (CMOS) technologies, have potential for the development of low-noise flexible real-time detection arrays for drug discovery and other testing. Finally, the fast response, stability, and label-free flexible fabrication of these sensors with ultrahigh sensitivity and selectivity clearly shows the potential of this tool for gaining information from genomics to proteomics to improve accurate molecular and even point-of-care clinical diagnosis.

Received: October 15, 2010
Published online: February 21, 2011

Keywords: aptamers · biosensors · molecular devices · nanotubes

[1] a) C. Sander, *Science* **2000**, *287*, 1977; b) J. Liu, Z. Cao, Y. Lu, *Chem. Rev.* **2009**, *109*, 1948; c) F. Patolsky, G. Zheng, C. M. Lieber, *Nat. Protoc.* **2006**, *1*, 1711; d) X. Fang, W. Tan, *Acc. Chem. Res.* **2010**, *43*, 48; e) T. G. Drummond, M. G. Hill, J. K. Barton, *Nat. Biotechnol.* **2003**, *21*, 1192.

[2] a) A. M. Ward, J. W. F. Catto, F. C. Hamdy, *Ann. Clin. Biochem.* **2001**, *38*, 633; b) C. Campagnolo, K. J. Meyers, T. Ryan, R. C. Atkinson, Y.-T. Chen, M. J. Scanlan, G. Ritter, L. J. Old, C. A. Batt, *J. Biochem. Biophys. Methods* **2004**, *61*, 283; c) E. M. Boon, J. E. Salas, J. K. Barton, *Nat. Biotechnol.* **2002**, *20*, 282; d) Y. Xiao, A. A. Lubin, A. J. Heeger, K. W. Plaxco, *Angew. Chem.* **2005**, *117*, 5592; *Angew. Chem. Int. Ed.* **2005**, *44*, 5456; e) Y. Jiang, X. Fang, C. Bai, *Anal. Chem.* **2004**, *76*, 5230; f) M. Löhndorf, U. Schlecht, T. Gronewold, A. Malave, M. Tewes, *Appl. Phys. Lett.* **2005**, *87*, 243902; g) J.-M. Nam, C. S. Thaxton, C. A. Mirkin, *Science* **2003**, *301*, 1884; h) G. Wu, R. H. Datar, K. M. Hansn, T. Thundat, R. J. Cote, A. Majumdar, *Nat. Biotechnol.* **2001**, *19*, 856; i) R. J. Chen, S. Bangsaruntip, K. A. Drouvalakis, N. W. S. Kam, M. Shim, Y. Li, W. Kim, P. J. Utz, H. Dai, *Proc. Natl. Acad. Sci. USA* **2003**, *100*, 4984; j) G. Zheng, F. Patolsky, Y. Cui, W. U. Wang, C. M. Lieber, *Nat. Biotechnol.* **2005**, *23*, 1294.

[3] a) F. Patolsky, G. Zheng, O. Hayden, M. Lakadamyali, X. Zhuang, C. M. Lieber, *Proc. Natl. Acad. Sci. USA* **2004**, *101*, 14017; b) B. R. Goldsmith, J. G. Coroneus, V. R. Khalap, A. A. Kane, G. A. Weiss, P. G. Collins, *Science* **2007**, *315*, 77.

[4] a) A. K. Feldman, M. L. Steigerwald, X. Guo, C. Nuckolls, *Acc. Chem. Res.* **2008**, *41*, 1731; b) X. Guo, J. P. Small, J. E. Klare, Y. Wang, M. S. Purewal, I. W. Tam, B. H. Hong, R. Caldwell, L. Huang, S. O'Brien, J. Yan, R. Breslow, S. J. Wind, J. Hone, P. Kim, C. Nuckolls, *Science* **2006**, *311*, 356.

[5] J. C. Genereux, J. K. Barton, *Chem. Rev.* **2010**, *110*, 1642.

[6] a) X. Guo, A. Whalley, J. E. Klare, L. Huang, S. O'Brien, M. Steigerwald, C. Nuckolls, *Nano Lett.* **2007**, *7*, 1119; b) X. Guo, A. A. Gorodetsky, J. Hone, J. K. Barton, C. Nuckolls, *Nat. Nanotechnol.* **2008**, *3*, 163.

[7] a) T. Takada, M. Fujitsuka, T. Majima, *Proc. Natl. Acad. Sci. USA* **2007**, *104*, 11179; b) M. Di Ventra, M. Zwolak, *Encycl. Nanosci. Nanotechnol.* **2004**, *2*, 475.

[8] a) A. D. Ellington, J. W. Szostak, *Nature* **1990**, *346*, 818; b) C. Tuerk, L. Gold, *Science* **1990**, *249*, 505.

[9] a) E. Baldrich, A. Restrepo, C. K. O'Sullivan, *Anal. Chem.* **2004**, *76*, 7053; b) K. Padmanabhan, K. P. Padmanabhan, J. D. Ferrara, J. E. Sadler, A. Tulinsky, *J. Biol. Chem.* **1993**, *268*, 17651.

[10] U. Schlecht, A. Malavé, T. Gronewold, M. Tewes, M. Löhndorf, *Anal. Chim. Acta* **2006**, *573-574*, 65.
[11] a) S.-P. Liu, S. H. Weisbrod, Z. Tang, A. Marx, E. Scheer, A. Erbe, *Angew. Chem.* **2010**, *122*, 3385; *Angew. Chem. Int. Ed.* **2010**, *49*, 3313; b) N. Kang, A. Erbe, E. Scheer, *New J. Phys.* **2008**, *10*, 023030.
[12] a) K. Maehashi, T. Katsura, K. Kerman, Y. Takamura, K. Matsumoto, E. Tamiya, *Anal. Chem.* **2007**, *79*, 782; b) H. R. Byon, H. C. Choi, *J. Am. Chem. Soc.* **2006**, *128*, 2188.
[13] M. D. Newton, J. F. Smalley, *Phys. Chem. Chem. Phys.* **2007**, *9*, 555.
[14] a) F. Patolsky, B. P. Timko, G. Yu, Y. Fang, A. B. Greytak, G. Zheng, C. M. Lieber, *Science* **2006**, *313*, 1100; b) Z. Li, Y. Chen, X. Li, T. I. Kamins, K. Nauka, R. S. Williams, *Nano Lett.* **2004**, *4*, 245; c) Z. Li, B. Rajendran, T. I. Kamins, X. Li, Y. Chen, R. S. Williams, *Appl. Phys. A* **2005**, *80*, 1257; d) P. E. Sheehan, L. J. Whitman, *Nano Lett.* **2005**, *5*, 803; e) P. R. Nair, M. A. Alam, *Nano Lett.* **2008**, *8*, 1281; f) B. R. Goldsmith, J. G. Coroneus, A. A. Kane, G. A. Weiss, P. G. Collins, *Nano Lett.* **2008**, *8*, 189.

